Shortest paths for efficient control of indirectly coupled qubits

Navin Khaneja,[1,*] Björn Heitmann,[2] Andreas Spörl,[2] Haidong Yuan,[1] Thomas Schulte-Herbrüggen,[2] and Steffen J. Glaser[2]
[1]*Division of Engineering and Applied Sciences, Harvard University, Cambridge, Massachusetts 02138, USA*
[2]*Department of Chemistry, Technische Universität München, Lichtenbergstrasse 4, D-85747 Garching, Germany*
(Received 1 September 2006; published 22 January 2007)

What is the time-optimal way of realizing quantum operations? Here, we show how important instances of this problem can be related to the study of shortest paths on the surface of a sphere under a special metric. Specifically, we provide an efficient synthesis of a controlled-NOT (CNOT) gate between qubits (spins $\frac{1}{2}$) coupled indirectly via Ising-type couplings to a third spin. Our implementation of the CNOT gate is significantly shorter than conventional approaches. The pulse sequences for efficient manipulation of our coupled spin system are obtained by explicit computation of geodesics on a sphere under the special metric. These methods are also used for the efficient synthesis of indirect couplings and of the Toffoli gate. We provide experimental realizations of the presented methods on a linear three-spin chain with Ising couplings.

DOI: 10.1103/PhysRevA.75.012322 PACS number(s): 03.67.Lx

I. INTRODUCTION

Quantum computation promises solutions to problems that are hard to solve by classical computers [1,2]. The efficient construction of quantum circuits that can solve interesting tasks is a fundamental challenge in the field [3,4]. Efficient construction of quantum circuits also reduces decoherence losses in physical implementations of quantum algorithms by reducing interaction time with the environment. Therefore finding time-optimal ways to synthesize unitary transformations from available physical resources is a problem of both fundamental and practical interest in quantum information processing. It has received significant attention, and time-optimal control of two coupled qubits [5–8] is now well understood. Recently, this problem has also been studied in the context of linearly coupled three-qubit topologies [9], where significant savings in implementation time of trilinear Hamiltonians were demonstrated over conventional methods. However, the complexity of the general problem of time optimal control of multiple qubit topologies is only beginning to be appreciated. The scope of these issues extends to broader areas of coherent spectroscopy and coherent control, where it is desirable to find time optimal ways to steer quantum dynamics between points of interest to minimize losses due to couplings to the environment [10,11].

One approach of effectively tackling this task is to map the problem of efficient synthesis of unitary transformations to the geometrical question of finding the shortest paths on the group of unitary transformations under a modified metric [3,5,9]. The optimal time variation of the Hamiltonian of the quantum system that produces the desired transformation is obtained by explicit computation of these geodesics. The metric enforces the constraints on the quantum dynamics that arise because only limited Hamiltonians can be realized. Such analogies between optimization problems related to steering dynamical systems with constraints and geometry have been well explored in areas of control theory [12,13] and sub-Riemannian geometry [14]. In this paper, we study in detail the metric and the geodesics that arise from the problem of efficient synthesis of couplings and quantum gates between indirectly coupled qubits in quantum information processing.

Synthesizing interactions between qubits that are indirectly coupled through intermediate qubits is a typical scenario in many practical implementations of quantum information processing and coherent spectroscopy. Examples include implementing two-qubit gates between distant spins on a spin chain [15,16] or using an electron spin to mediate couplings between two nuclear spins [17]. Multidimensional NMR experiments require synthesis of couplings between indirectly coupled qubits in order to generate high-resolution spectral information [18]. The synthesis of two-qubit gates between indirectly coupled qubits tends to be expensive in terms of time for their implementation. This is because such gates are conventionally constructed by concatenating two-qubit operations on directly coupled spins. Lengthy implementations lead to relaxation losses and poor fidelity of the gates. In this paper, we develop methods for efficiently manipulating indirectly coupled qubits. In particular, we study the problem of efficient synthesis of couplings and controlled NOT (CNOT) gates between indirectly coupled spins and demonstrate significant improvement in implementation time over conventional methods. We also show how these methods can be used for efficient synthesis of other quantum logic gates like, for example, a Toffoli gate [19–21] on a three-qubit topology, with qubits 1 and 3 indirectly coupled through qubit 2. Experimental implementations of the main ideas are demonstrated for a linear three-spin chain with Ising couplings in solution state NMR.

II. THEORY

A geodesic is the shortest path between two points in a curved space. Under the standard Euclidean metric $(dx)^2+(dy)^2+(dz)^2$, the geodesics connecting any two points in a plane are straight lines and geodesics on a sphere are segments of great circles. In this paper, we study the geodesics on a sphere under the metric $g=\frac{(dx)^2+(dz)^2}{y^2}$ (note on the unit

*Corresponding author. Electronic address: navin@hrl.harvard.edu

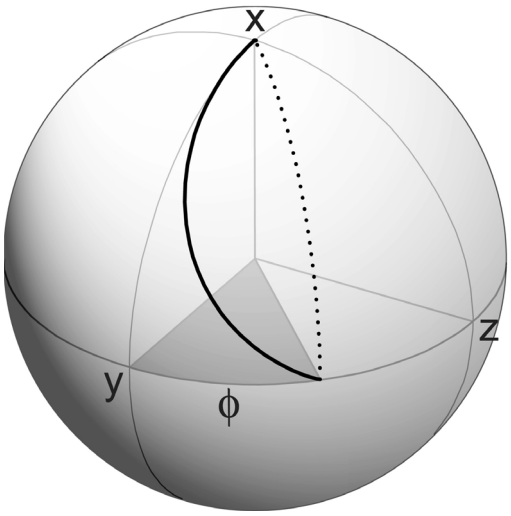

FIG. 1. The solid curve in Fig. 1 depicts the shortest path connecting the north pole $(1,0,0)$ to a point $(0,\cos\phi,\sin\phi)$ under the metric g. The dashed curve is the geodesic under the standard metric and represents a segment of a great circle.

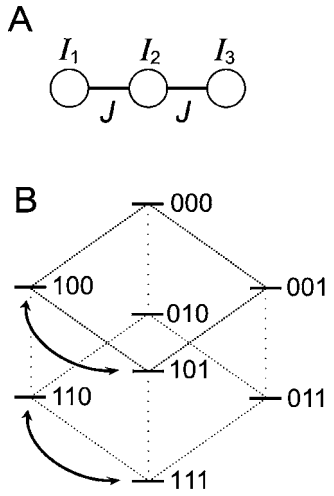

FIG. 2. (A) Coupling topology where the first qubit (I_1) and third qubit (I_3) are coupled only indirectly via the second qubit (I_2) with coupling constants $J_{12}=J_{23}=J$. (B) Schematic energy-level diagram for the spin system in a static magnetic field in the z direction, which determines the quantization axis. The Zeeman energy of a state $|b_1b_2b_3\rangle$ is $\Sigma_{k=1}^{3}(\frac{1}{2}-b_k)\omega_i$, where ω_k is the Larmor frequency of spin I_k; $b_k=1$ and 0 correspond to the low- and high-energy eigenstates of the angular momentum operator along the z direction. The schematic representation in (B), corresponds to the case $\omega_1\approx\omega_3$. The coupling term [Eq. (2)] results in an additional shift of the states $|000\rangle$ and $|111\rangle$ by πJ and of the states $|010\rangle$ and $|101\rangle$ by $-\pi J$ (not visible in the figure because $|J|\ll|\omega_k|$. The effect of the CNOT(1, 3) unitary transformation is indicated by arrows.

sphere $y^2=1-x^2-z^2$). The solid curve in Fig. 1 depicts the shortest path connecting the north pole $(1,0,0)$ to a point $(0,\cos\phi,\sin\phi)$, under the metric g. The dashed curve is the geodesic under the standard metric and represents a segment of a great circle. For $\phi=\frac{\pi}{4}$, the length L of the geodesic under g is 0.627π (as opposed to $\frac{\pi}{2}$ under the standard metric). We call this metric g, the quantum gate design metric. If w represents the complex number $w=x+iz$, then the quantum gate design metric can be written as

$$g=\frac{|dw|^2}{1-|w|^2}. \tag{1}$$

It has marked similarity to the Poincaré metric $\frac{|dw|^2}{(1-|w|^2)^2}$ in Hyperbolic geometry [22], defined on the unit disk.

We show how problems of efficiently steering quantum dynamics of coupled qubits can be mapped to the study of shortest paths under the metric g. Computing geodesics under g helps us to develop techniques for efficient synthesis of transformations in the 63-dimensional space of (special) unitary operators on three coupled qubits.

We consider a linear Ising chain, consisting of three coupled qubits (spins 1/2) with coupling constants $J_{12}=J_{23}=J$ and $J_{13}=0$ [see Fig. 2(A)]. The coupling Hamiltonian between the qubits is given by [18]

$$\mathcal{H}_c=2\pi J(I_{1z}I_{2z}+I_{2z}I_{3z}), \tag{2}$$

where, e.g., $I_{1z}=\frac{1}{2}\sigma_z\otimes\mathbf{1}_{2\times2}\otimes\mathbf{1}_{2\times2}$, σ_z is a Pauli spin operator, and $\mathbf{1}_{2\times2}$ is the 2×2 unit matrix [18].

The spin system is controlled by local unitary operations on individual qubits, which we assume take negligible time compared to the evolution of couplings (strong pulse limit) [5]. The strength of couplings limits the time it takes to synthesize quantum logical gates between coupled qubits. We seek to find the optimal way to perform local control on qubits in the presence of evolution of couplings to perform fastest possible synthesis of quantum logic gates. For directly coupled qubits, this problem has been solved. For example, a CNOT(1,2) gate which inverts spin 2 conditioned on the state of spin 1 requires a minimum of $0.5J^{-1}$ [5]. Here, we focus on the problem of synthesizing the CNOT(1,3) gate between indirectly coupled spins. Figure 2(B) shows the energy-level diagram for the CNOT(1,3) operation, where the state of qubit 3 is inverted if qubit 1 is in a lower energy state, i.e., in state 1. In the literature, various constructions of CNOT(1,3) gates have been considered with durations ranging from $3.5J^{-1}$ to $2.5J^{-1}$ [23]. The main result of this paper is that the CNOT(1,3) gate can be realized in only $\frac{2l}{\pi J}$ units of time, where l is the length of the geodesic under the metric g for $\phi=\frac{\pi}{4}$ as depicted in Fig. 1. This is significantly faster than the best known conventional approach. The new pulse sequence for the CNOT(1,3) gate is based on the sequence element shown in Fig. 3(A).

The main ideas for discovering the new efficient pulse sequence are as follows. The unitary propagator for a CNOT gate is

$$\text{CNOT}(1,3)=\exp\left\{-i\frac{\pi}{2}\left(2I_{1z}I_{3x}-I_{1z}-I_{3x}+\frac{1}{2}\mathbf{1}\right)\right\}, \tag{3}$$

where $\mathbf{1}$ is the identity operator and $I_{k\alpha}$ is 1/2 times the Pauli-spin operator on qubit k with $\alpha\in\{x,y,z\}$ [18]. Since we assume that local operations take negligible time, we consider the synthesis of the unitary operator

$$\mathcal{U}_{13}^{s} = \exp\left\{-i\frac{\pi}{2}(I_{1z} + I_{3z} + 2I_{1z}I_{3z})\right\}, \tag{4}$$

which is locally equivalent to the CNOT(1,3) operator but symmetric in qubits 1 and 3.

For synthesizing $\mathcal{U}_{13}^{s}$, we seek to engineer a time varying Hamiltonian that transforms the various quantum states in the same way as $\mathcal{U}_{13}^{s}$ does. The unitary transformation $\mathcal{U}_{13}^{s}$ transforms the operators $I_{1\alpha}$ and $I_{3\alpha}$ (with the indices $\alpha \in \{x,y\}$) to $-2I_{1\alpha}I_{3z}$ and $-2I_{1z}I_{3\alpha}$, respectively. Since $\mathcal{U}_{13}^{s}$ treats the operators $I_{1x,1y}$ and $I_{3x,3y}$ symmetrically, we seek to construct the propagator $\mathcal{U}_{13}^{s}$ by a time varying Hamiltonian that only involves the evolution of Hamiltonian $\mathcal{H}_c$ and single qubit operations on the second spin. The advantage of restricting to only these two control actions is that it is then sufficient to engineer a pulse sequence for steering just the initial state I_{1x} to its target operator $-2I_{1x}I_{3z}$. Other operators in the space $\{I_{1\alpha}, I_{3\beta}, 2I_{1\alpha}I_{3\beta}\}$ are then constrained to evolve to their respective targets (as determined by the action of $\mathcal{U}_{13}^{s}$). Our approach can be broken down into the following steps:

(I) In a first step, the problem of efficient transfer of I_{1x} to $-2I_{1x}I_{3z}$ in the 63-dimensional operator space of three qubits is reduced to a problem in the six-dimensional operator space $\mathcal{S}$, spanned by the set of operators I_{1x}, $2I_{1y}I_{2z}$, $2I_{1y}I_{2x}$, $4I_{1y}I_{2y}I_{3z}$, $4I_{1y}I_{2z}I_{3z}$, and $2I_{1x}I_{3z}$. (The numerical factors of 2 and 4 simplify the commutation relations among the operators.) The subspace $\mathcal{S}$ is the lowest dimensional subspace in which the initial state I_{1x} and the target state $-2I_{1x}I_{3z}$ are coupled by $\mathcal{H}_c$ and the single qubit operations on the second spin.

(II) In a second step, the six-dimensional problem is decomposed into two independent (but equivalent) four-dimensional time optimal control problems.

(III) Finally, it is shown that the solution of these time optimal control problems reduces to computing shortest paths on a sphere under the modified metric g.

In step (I), any operator in the six-dimensional subspace $\mathcal{S}$ of the 63-dimensional operator space is represented by the coordinates $x=(x_1,x_2,x_3,x_4,x_5,x_6)$, where the coordinates are given by the following six expectation values: $x_1=\langle I_{1x}\rangle$, $x_2=\langle 2I_{1y}I_{2z}\rangle$, $x_3=\langle 2I_{1y}I_{2x}\rangle$, $x_4=\langle 4I_{1y}I_{2y}I_{3z}\rangle$, $x_5=\langle 4I_{1y}I_{2z}I_{3z}\rangle$, and $x_6=-\langle 2I_{1x}I_{3z}\rangle$. In the presence of the coupling $\mathcal{H}_c$, a rotation of the second qubit around the y axes [affected by a rf Hamiltonian $\mathcal{H}_A=u_A(t)\pi JI_{2y}$] couples the first four components $x_A=(x_1,x_2,x_3,x_4)^t$ of the vector x. In the presence of $\mathcal{H}_c$, a rotation around the x axes [affected by a rf Hamiltonian $\mathcal{H}_B=u_B(t)\pi JI_{2x}$] mixes the last four components $x_B=(x_3,x_4,x_5,x_6)^t$ of the vector x. Under x or y pulses applied to the second qubit in the presence of $\mathcal{H}_c$, the equations of motion for the column vectors x_A and x_B have the same form:

$$\frac{dx_{A,B}}{dt} = \pi J\begin{pmatrix} 0 & -1 & 0 & 0 \\ 1 & 0 & -u_{A,B} & 0 \\ 0 & u_{A,B} & 0 & -1 \\ 0 & 0 & 1 & 0 \end{pmatrix} x_{A,B}. \tag{5}$$

Since evolution of x_A and x_B is equivalent, it motivates the following sequence of transformations that treats the two systems symmetrically and steers I_{1x} [corresponding to $x_A=(1,0,0,0)^t$] to $-2I_{1x}I_{3z}$ [corresponding to $x_B=(0,0,0,1)^t$]: (i) transformation from $(1,0,0,0)$ to $\left(0,x_2',x_3',\frac{1}{\sqrt{2}}\right)$ in subsystem A with $\sqrt{x_2'^2+x_3'^2}=\frac{1}{\sqrt{2}}$; (ii) transformation from $\left(0,x_2',x_3',\frac{1}{\sqrt{2}}\right)$ to $\left(0,0,\frac{1}{\sqrt{2}},\frac{1}{\sqrt{2}}\right)$ in subsystem A [corresponding to

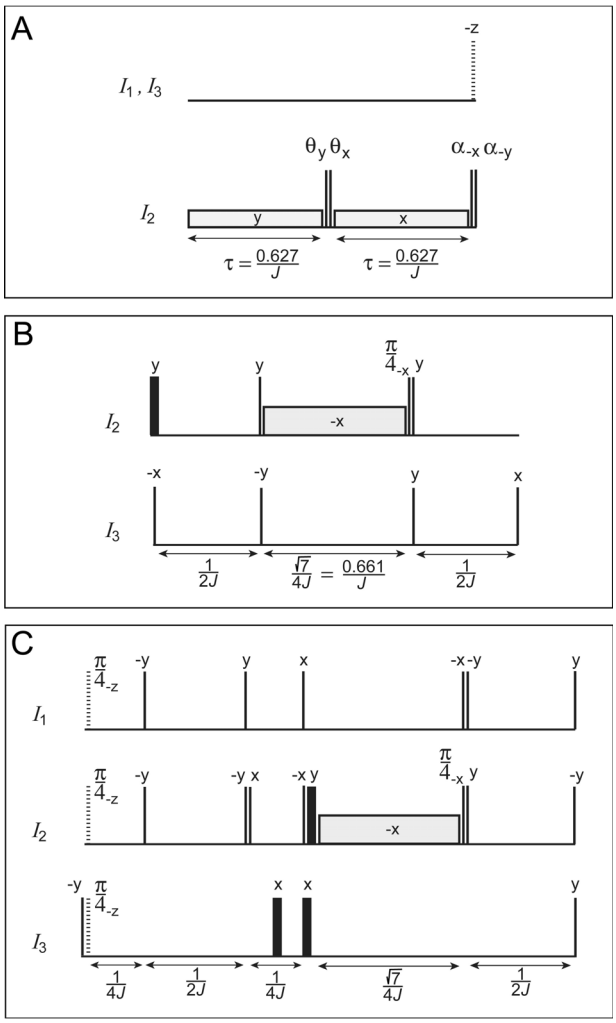

FIG. 3. Efficient pulse sequences based on sub-Riemannian geodesics for the implementation of $\mathcal{U}_{13}=\exp\{-i\frac{\pi}{2}2I_{1z}I_{3z}\}$ (A), $\sqrt{\mathcal{U}_{13}}=\exp\{-i\frac{\pi}{4}2I_{1z}I_{3z}\}$ (B), simulating coupling evolution by angles $\frac{\pi}{2}$ (A) and $\frac{\pi}{4}$ (B) between indirectly coupled qubits, and of a Toffoli gate (C). Qubits I_1, I_2, and I_3 are assumed to be on-resonance in their respective rotating frames. Narrow and wide vertical bars correspond to hard pulses with flip angles $\pi/2$ and π, respectively, if no other flip angle is indicated. Rotations around the z axis are represented by dashed bars. The unitary operator $\mathcal{U}_{13}$, which is locally equivalent to the CNOT(1,3) gate, is synthesized by sequence (A) in a total time $T_C^*=2\tau=1.253J^{-1}$. The amplitude of the weak pulses (represented by gray boxes) with a duration of $\tau=0.627J^{-1}$ is $\nu_a=uJ/2=0.52J$. The hard-pulse flip angles $\theta=31.4°$ and $\alpha=180°-\theta=148.6°$. Sequence (B) of total duration $(4+\sqrt{7})/4J^{-1}=1.66J^{-1}$ synthesizes the propagator $\sqrt{\mathcal{U}_{13}}$. The amplitude of the weak pulse (gray box) with a duration of $\sqrt{7}/4J^{-1}=0.661J^{-1}$ is $\nu_w=3J/\sqrt{7}=1.134J$. Pulse sequence (C) realizes the Toffoli gate in a total time $(6+\sqrt{7})/4J^{-1}=2.16J^{-1}$. The sequence is based on the sequence for $\sqrt{\mathcal{U}_{13}}$ and a weak pulse with the same amplitude and duration as in sequence (B).

$\left(\frac{1}{\sqrt{2}},\frac{1}{\sqrt{2}},0,0\right)$ in subsystem B]; (iii) transformation from $\left(\frac{1}{\sqrt{2}},\frac{1}{\sqrt{2}},0,0\right)$ to $\left(\frac{1}{\sqrt{2}},x_3',x_2',0\right)$ in subsystem B; (iv) transformation from $\left(\frac{1}{\sqrt{2}},x_3',x_2',0\right)$ to $(0,0,0,1)$ in subsystem B.

Transformations (ii) and (iii) represent local y and x rotations of the second spin, respectively, and take a negligible amount of time in the strong pulse limit: Transformation (ii) is accomplished by a local θ_y rotation of the second qubit, i.e., a strong pulse with flip angle θ (where $\tan\theta=x_2'/x_3'$) and phase y. Similarly, transformation (iii) can be accomplished by a local θ_x rotation applied to the second qubit. Because of the symmetry of the two subsystems A and B, the transformations (i) and (iv) are equivalent and take the same amount of time with (iv) being the time-reversed transformation of (i) and x_5 and x_6 replacing x_2 and x_1, respectively. Hence the problem of finding the fastest transformations (i)–(iv), reduces to a time optimal control problem in the four-dimensional subspace A, asking for the choice of $u_A(t)$ that achieves transfer (i) in the minimum time [step (II)].

In step (III), this optimal control problem is reduced to the shortest path problem on a sphere (under metric g) described in the beginning of the section (see Fig. 1). The key ideas are as follows. Let $x(t)=x_1(t)$, $y(t)=\sqrt{x_2^2(t)+x_3^2(t)}$ and $z(t)=x_4(t)$. Since $u_A(t)$ can be made large, we can control the angle $\tan\theta(t)=\frac{x_2(t)}{x_3(t)}$ arbitrarily fast in the strong pulse limit. With the new variables $(x(t),y(t),z(t))$, Eq. (5) reduces to

$$\frac{d}{dt}\begin{bmatrix}x\\y\\z\end{bmatrix}=\pi J\begin{bmatrix}0 & -\sin\theta(t) & 0\\ \sin\theta(t) & 0 & -\cos\theta(t)\\ 0 & \cos\theta(t) & 0\end{bmatrix}\begin{bmatrix}x\\y\\z\end{bmatrix}. \tag{6}$$

In this system, the goal of achieving the fastest transformation (a) corresponds to finding the optimal angle $\theta(t)$ such that $(1,0,0)$ is steered to $\left(0,\frac{1}{\sqrt{2}},\frac{1}{\sqrt{2}}\right)$ in minimum time. The time of transfer τ can be written as $\int_0^\tau\sqrt{\sin^2\theta(t)+\cos^2\theta(t)}dt$. Substituting for $\sin\theta(t)$ and $\cos\theta(t)$ from Eq. (6), this reduces to

$$\frac{1}{\pi J}\int\underbrace{\sqrt{\frac{(\dot{x})^2+(\dot{z})^2}{y^2}}}_{L}dt. \tag{7}$$

Thus minimizing τ amounts to computing the geodesic under the metric g given in Eq. (1). We first characterize these geodesics connecting $(1,0,0)$ to $(0,\cos\phi,\sin\phi)$, for general ϕ and then evaluate the geodesic length for the specific $\phi=\frac{\pi}{4}$ of interest. With the Lagrange function L defined in Eq. (7) and using $y^2=1-x^2-z^2$, to constrain the trajectory to the sphere, the Euler-Lagrange equations for the geodesic take the form

$$\frac{d}{dt}\left(\frac{\partial L}{\partial\dot{x}}\right)=\frac{\partial L}{\partial x};\quad \frac{d}{dt}\left(\frac{\partial L}{\partial\dot{z}}\right)=\frac{\partial L}{\partial z}. \tag{8}$$

Note, by definition, L is constant along the trajectories and takes the value 1. This gives

$$\frac{d}{dt}\left(\frac{\dot{x}}{y^2}\right)=L^2\frac{x}{y^2};\quad \frac{d}{dt}\left(\frac{\dot{z}}{y^2}\right)=L^2\frac{z}{y^2}, \tag{9}$$

which implies that

$$\frac{d}{dt}\left(\frac{\dot{x}z-\dot{z}x}{y^2}\right)=0. \tag{10}$$

The Euler-Lagrange equations imply that along geodesic curves, $\frac{\dot{x}z-\dot{z}x}{y^2}=f$ is a constant. Substituting back in Eq. (9) gives

$$\frac{d}{dt}\left(\frac{\dot{x}}{y}\right)=-f\frac{\dot{z}}{y};\quad \frac{d}{dt}\left(\frac{\dot{z}}{y}\right)=f\frac{\dot{x}}{y}, \tag{11}$$

which implies that $\frac{\dot{x}}{y}=A_0\cos(ft+\gamma)$ and $\frac{\dot{z}}{y}=A_0\sin(ft+\gamma)$. For geodesics originating from $(1,0,0)$, at time $t=0$, we have $\frac{\dot{z}}{y}=0$ (for f to be finite) and hence $\gamma=0$. This implies from Eq. (6) that $A_0=\pi J$ and $\theta(t)=ft-\frac{\pi}{2}$. Now differentiating the expression $\frac{x_2}{x_3}(t)=\tan\left(ft-\frac{\pi}{2}\right)$ gives $u_A(t)=\frac{1}{\pi J}\left(-f+\frac{\dot{z}x-\dot{x}z}{y^2}\right)$. Along geodesic curves, $\frac{\dot{z}x-\dot{x}z}{y^2}$ is constant, implying that in Eq. (5), time optimal $u_A(t)=u$ is constant. We now simply search numerically for this constant u and the corresponding τ that will perform transformation (i) in system (5). From all feasible (u,τ) pairs, we choose the one with smallest τ. This gives $\tau=0.627J^{-1}$ and $u_A(t)=u_B(t)=u=1.04$. Evolving Eq. (5) for time τ with $u=1.04$ results in $\theta(\tau)=\tan^{-1}\frac{x_2'}{x_3'}=0.5476$. The optimal flip angle for the transformations (i) and (iv) is therefore $\theta(\tau)=0.5476$. We drop the argument τ in the subsequent text and use θ to denote $\theta(\tau)$. With this, the total unitary operator $\mathcal{U}_{13}^g$, corresponding to the transformations (i)–(iv) can be written in the form

$$\mathcal{U}_{13}^g=\Pi_x\exp\{-i\theta I_{2x}\}\exp\{-i\theta I_{2y}\}\Pi_y \tag{12}$$

with $\Pi_{x,y}=\exp\{-i\pi J\tau[2I_{1z}I_{2z}+2I_{2z}I_{3z}+uI_{2x,2y}]\}$. The pulse sequence for the implementation of $\mathcal{U}_{13}^g$ is evident from Eq. (12) and consists of a constant y pulse on spin 2 of amplitude $\nu_a=uJ/2=0.52J$ for a duration of $\tau=0.627J^{-1}$ followed by a y pulse and then a x pulse each of flip angle $\theta=0.5476$ (corresponding to 31.4°) on spin 2, both of negligible duration. Finally, we apply a constant x pulse on spin 2 of duration $\tau=0.627J^{-1}$ and amplitude $0.52J$. The overall duration for the implementation of $\mathcal{U}_{13}^g$ is $T=2\tau=1.253J^{-1}$.

We now show that $\mathcal{U}_{13}^g$ is locally equivalent to $\mathcal{U}_{13}^s$ [and hence to the CNOT(1,3) gate]. Therefore the CNOT(1,3) gate can also be implemented in a time $T=2\tau=1.253J^{-1}$. Let $\mathcal{I}_{1,3}$ denote the subspace spanned by the operators $\{I_{1\alpha},I_{3\beta},I_{1\alpha}I_{3\beta}\}$ with independent $\alpha,\beta\in\{x,y,z\}$ and $\mathcal{I}_2$ denote the space spanned by operators $\{I_{2\alpha}\}$. It can be explicitly verified that by construction $\mathcal{U}_{13}^g$ maps $\mathcal{I}_{1,3}$ to itself and acts identically as $\mathcal{U}_{13}^s$. This constrains $\mathcal{U}_{13}^g$ up to a local transformation on the space $\mathcal{I}_{1,3}\otimes\mathcal{I}_2$. We can therefore find local transformations U_a^{loc}, U_b^{loc}, and U_c^{loc} such that

$$\mathrm{CNOT}(1,3)=U_c^{loc}U_b^{loc}\mathcal{U}_{13}^gU_a^{loc}. \tag{13}$$

These local transformations are readily computed to equal $U_a^{loc}=\exp\{-i\frac{\pi}{2}I_{3y}\}$, $U_b^{loc}=\exp\{i(\pi-\theta)I_{2y}\}\exp\{i(\pi$

$-\theta)I_{2x}\}\exp\{i\frac{\pi}{2}(I_{1z}+I_{3z})\}$, and $U_c^{loc}=\exp\{-i\frac{\pi}{2}(I_{1z}-I_{3z})\}\times\exp\{-i\frac{\pi}{2}I_{3x}\}$. Furthermore, the propagator

$$\mathcal{U}_{13}=\exp\left\{-i\frac{\pi}{2}(2I_{1z}I_{3z})\right\}=U_b^{loc}\mathcal{U}_{13}^g, \tag{14}$$

representing a $\frac{\pi}{2}$ rotation under an effective 1-3 Ising coupling can also be generated in time $T=1.253J^{-1}$.

Until now we have assumed that the coupling between qubits 1 and 3 is zero. The methods presented here can be extended to account for the nonzero coupling between qubits 1 and 3. The main ideas are as follows. We have computed the minimum time to synthesize the propagator $\exp\{-i\frac{\pi}{2}2I_{1z}I_{3z}\}$ assuming $J_{13}=0$. Similar computations can be used to find the minimum time $\tau(\gamma)$ for the propagator $\exp\{-i\frac{\pi}{2}\gamma 2I_{1z}I_{3z}\}$ for $0<\gamma<1$ for $J_{13}=0$. Since the synthesis of this transformation only involves local rotations on the second qubit, the net propagator (taking into account the evolution of a nonzero coupling J_{13} between spin 1 and 3) is

$$\exp\left\{-i\frac{\pi}{2}[\gamma+2J_{13}\tau(\gamma)]2I_{1z}I_{3z}\right\}. \tag{15}$$

Now γ can be chosen such that $\gamma+2J_{13}\tau(\gamma)=1$.

The condition $J_{12}=J_{23}=J$ can also be relaxed. Observe that we can decompose the Hamiltonian $\mathcal{H}_c=2\pi(J_{12}I_{1z}I_{2z}+J_{23}I_{2z}I_{3z})$, as $2\pi J^+(I_{1z}I_{2z}+I_{2z}I_{3z})+2\pi J^-(I_{1z}I_{2z}-I_{2z}I_{3z})$, where $J^+=\frac{J_{12}+J_{23}}{2}$ and $J^-=\frac{J_{12}-J_{23}}{2}$. In the interaction frame of the rf irradiation on the second qubit, the Hamiltonians $I_{1z}I_{2z}+I_{2z}I_{3z}$ and $I_{1z}I_{2z}-I_{2z}I_{3z}$ commute for all times. Hence the problem of unequal couplings J_{12} and J_{23} can be reduced to two independent problems with equal coupling strength J^+ and J^-, respectively. Therefore finding optimal time varying excitation on the second qubit that produces a CNOT(1,3) gate, for the general coupling Hamiltonian $\mathcal{H}_c=2\pi(J_{12}I_{1z}I_{2z}+J_{23}I_{2z}I_{3z}+J_{13}I_{1z}I_{3z})$ can be approached based on the methods presented here. We plan to investigate this in detail in the future.

The methods developed above can also be used for efficient construction of trilinear propagators. This problem has been studied in detail in [9]. The main results of [9] become transparent in terms of geodesics under the metric g. Consider the propagator $\mathcal{U}_{zyz}(\kappa)=\exp\{-i2\pi\kappa I_{1z}I_{2y}I_{3z}\}$. To synthesize this propagator, we again seek to efficiently steer the various states between points as they would transform under $U_{zyz}(\kappa)$. For example, I_{1x} is transferred to $I_{1x}\cos\kappa+\sin\kappa 4I_{1y}I_{2y}I_{3z}$. Consider again the four-dimensional operator space A defined exactly as before. The goal now is to steer the initial vector x_A from the initial state $(1,0,0,0)$ to $(\cos\kappa,0,0,\sin\kappa)$ in Eq. (5). This in the transformed system Eq. (6), reduces to steering (x,y,z) from $(1,0,0)$ to $(\cos\kappa,0,\sin\kappa)$. The geodesics for this problem have already been characterized. The length of the geodesic that maps $(1,0,0)$ to $(\cos\kappa,0,\sin\kappa)$ under the metric g is $\pi\frac{\sqrt{\kappa(4-\kappa)}}{2}$ and leads to a minimum time of $\tau(\kappa)$ of [9],

$$\tau(\kappa)=\frac{\sqrt{\kappa(4-\kappa)}}{2J}. \tag{16}$$

The time optimal $u_A(t)$ in Eq. (5) is again constant and the resulting unitary propagator is locally equivalent to $\mathcal{U}_{zyz}(\kappa)$. Since all trilinear propagators $U_{\alpha\beta\gamma}$ are locally equivalent, we get efficient ways of synthesizing all these propagators.

III. DISCUSSION

We now compare the efficient synthesis of the CNOT(1,3) gate presented above with some conventional methods. The simplest approach (pulse sequence C1) to implement an indirect CNOT gate between spin 1 and 3 involves swapping the state of spins 1 and 2 followed by a CNOT(2,3) gate and a final swap between 1 and 2, resulting in CNOT(1,3) =SWAP(1,2) CNOT(2,3) SWAP(1,2). The minimum time for implementing a CNOT gate between directly coupled spins 2 and 3 is $0.5J^{-1}$ [5] and each SWAP operation takes $1.5J^{-1}$ units of time, resulting in a total implementation time of $3.5J^{-1}$ [23].

Since we assume that local operations take negligible time, the central step in synthesizing a CNOT(1,3) gate is the construction of the unitary operator $\mathcal{U}_{13}=\exp\{-i\frac{\pi}{2}2I_{1z}I_{3z}\}$. The standard method of synthesizing such an operator creates a trilinear propagator $\mathcal{U}_{zzy}=\exp\{-i\frac{\pi}{2}4I_{1z}I_{2z}I_{3y}\}$ and uses the following identity: $\mathcal{U}_{13}=\exp\{-iH_1\}\mathcal{U}_{zzy}\exp\{iH_1\}$, and

$$\mathcal{U}_{zzy}=\exp\{-iH_2\}\exp\left\{-i\frac{\pi}{2}2I_{1z}I_{2y}\right\}\exp\{iH_2\}, \tag{17}$$

where $H_1=\frac{\pi}{2}2I_{2z}I_{3x}$ and $H_2=\frac{\pi}{2}2I_{2x}I_{3y}$. Overall, this takes $2.5J^{-1}$ units of time [23], resulting in a realization pulse sequence C2 of the CNOT(1,3) gate that takes only 71.4% of the time required for the implementation, pulse sequence C1.

The time to synthesize the CNOT(1,3) gate can thus be shortened by reducing the time to synthesize the propagator $\mathcal{U}_{zzy}$. We can use a more efficient synthesis of these trilinear propagators discussed in [9] to further improve the efficiency of synthesis of the CNOT(1,3) gate. Note

$$\mathcal{U}_{zzy}=\exp\left\{i\frac{\pi}{2}I_{2z}\right\}\exp\{-iH_{3x}\}\exp\{-i2H_{3y}\}\exp\{iH_{3x}\}, \tag{18}$$

where $H_{3\alpha}=\frac{\pi}{4}(2I_{1z}I_{2\alpha}+2I_{2\alpha}I_{3y})$, with $\alpha\in\{x,y,z\}$. This reduces the implementation time of $\mathcal{U}_{zzy}$ to J^{-1} and of CNOT(1,3) to $2J^{-1}$ (pulse sequence C3). This time can be even further reduced by using the fact that the shortest time to produce the propagator $\mathcal{U}_{zzy}$ is given by $\sqrt{3}/(2J)$ [9] [see Eq. (16)] and uses the identity

$$\mathcal{U}_{zzy}=\exp\left\{i\frac{\pi}{2}I_{2z}\right\}\exp\left\{-i\sqrt{3}\frac{\pi}{2}\left(2I_{1z}I_{2x}+2I_{2x}I_{3y}+\frac{2}{\sqrt{3}}I_{2z}\right)\right\}\times\exp\left\{-i\frac{3\pi}{2}I_{2z}\right\}. \tag{19}$$

This implementation then results in a total time of $(2+\sqrt{3})/(2J)=1.866/J$ (pulse sequence C4) for the CNOT(1,3)

TABLE I. Duration τ_C of various implementations of the CNOT(1,3) gate.

Pulse sequence	τ_C (units of J^{-1})	Relative duration (%)
Sequence 1 (C1)	3.5	100
Sequence 2 (C2)	2.5	71.4
Sequence 3 (C3)	2.0	57.1
Sequence 4 (C4)	1.866	53.3
Sequence 5 (C5)	1.253	38.8

gate. The implementation, pulse sequence C5, proposed here is still significantly shorter than this. The implementation times under various strategies are summarized in Table I.

We now show how efficient implementation of trilinear propagators can also be used for efficient construction of other quantum gates like a controlled NOT (Toffoli) gate on spin 3 conditioned on the state of spin 1 and 2 for the linear spin chain architecture, cf. Table II. The decomposition given in [21] is based on four CNOT gates (requiring $0.5J^{-1}$ each) between directly coupled qubits and two CNOT gates between indirectly coupled qubits. Hence using a SWAP-based implementation of the CNOT(1,3) gates (pulse sequence C1), each of which requires $3.5J^{-1}$, the total duration of the Toffoli gate would be $9J^{-1}$ (Toffoli gate pulse sequence T1). With the most efficient implementation of the CNOT(1,3) (gate pulse sequence C5), each of which requires $1.253J^{-1}$, the decomposition [21] has a total duration of about $4.5J^{-1}$ (gate pulse sequence T2). The Sleator-Weinfurter construction [20] of the Toffoli gate is based on two CNOT operations between directly coupled qubits, two unitary operations which are locally equivalent to the evolution of the coupling between directly coupled qubits, each of duration $0.25J^{-1}$ and one unitary operator which is locally equivalent to $\sqrt{\mathcal{U}_{13}}=\exp\left(-i\frac{\pi}{4}2I_{1z}I_{3z}\right)$. A naive approach for synthesizing $\sqrt{\mathcal{U}_{13}}$ using SWAP operations has a duration of $3.25J^{-1}$, resulting in a total duration of the Toffili gate of $4.75J^{-1}$ (gate pulse sequence T3). Based on the optimal synthesis of trilinear propagators [9] $\sqrt{\mathcal{U}_{13}}$ can be implemented in $\frac{4+\sqrt{7}}{4J}=1.66J^{-1}$ units of time [see Fig. 3(B)]. The main identity used is $\sqrt{\mathcal{U}_{13}}=\exp\left(-i\frac{\pi}{2}2I_{2z}I_{3y}\right)\exp\left(-i\frac{\pi}{4}4I_{1z}I_{2z}I_{3z}\right)\exp\left(i\frac{\pi}{2}2I_{2z}I_{3y}\right)$. This reduces the overall duration of the Sleator-Weinfurter construction to $3.16J^{-1}$ (gate pulse sequence T4).

Here, we present even shorter implementations of the Toffoli gate, the propagator of which is given by U_{toff}

TABLE II. Duration τ_T of various implementations of the Toffoli gate.

Pulse sequence	τ_T (units of J^{-1})	Relative duration (%)
Sequence 1 (T1)	9.0	100
Sequence 2 (T2)	4.5	50
Sequence 3 (T3)	4.75	52.8
Sequence 4 (T4)	3.16	35.1
Sequence 5 (T5)	2.57	28.6
Sequence 6 (T6)	2.16	24.0

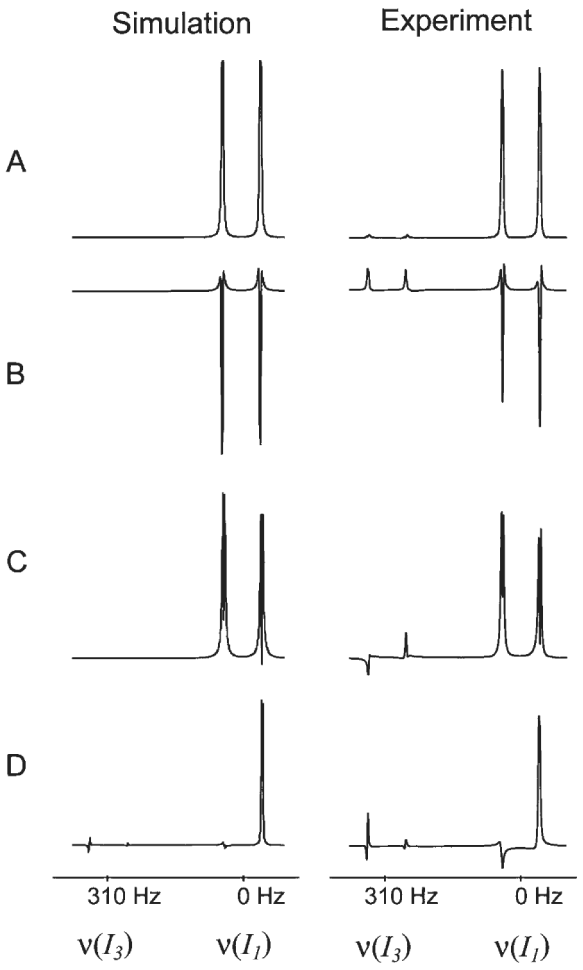

FIG. 4. Simulated (left) and experimental (right) ^{1}H spectra of the amino moiety of ^{15}N acetamide with $J_{12}=-87.3$ Hz, $J_{23}=-88.8$ Hz, and $J_{13}=2.9$ Hz. Starting from thermal equilibrium, in all experiments the state $\rho_A=I_{1x}$ was prepared by saturating spins I_2 and I_3 and applying a 90°_y pulse to spin I_1, where ρ_A is the traceless part of the density operator [18]. (A) Spectrum corresponding to $\rho_A=I_{1x}$, (B) spectrum obtained after applying the propagator $\mathcal{U}_{13}=\exp\left\{-i\frac{\pi}{2}2I_{1z}I_{3z}\right\}$ to ρ_A, (C) resulting spectrum after applying the propagator $\sqrt{\mathcal{U}_{13}}=\exp\left\{-i\frac{\pi}{4}2I_{1z}I_{3z}\right\}$ to ρ_A, (D) spectrum after applying the Toffoli gate to ρ_A.

$=\exp\left\{-i\pi\left(\frac{1}{2}\mathbf{1}-I_{1z}\right)\left(\frac{1}{2}\mathbf{1}-I_{2z}\right)\left(\frac{1}{2}\mathbf{1}+I_{3x}\right)\right\}$. Neglecting terms in the Hamiltonian corresponding to multiples of the unit operator $\mathbf{1}$ and to single spin operations (as these take negligible time to synthesize), the effective Hamiltonian for the Toffoli gate is locally equivalent to $H_{toff}=\frac{\pi}{4}\{2I_{1z}I_{2z}+2I_{2z}I_{3x}+2I_{1z}I_{3x}+4I_{1z}I_{2z}I_{3x}\}$. The synthesis of $\frac{\pi}{4}\{2I_{1z}I_{2z}+2I_{2z}I_{3x}\}$ is achieved by evolution under the direct couplings for $(4J)^{-1}$ units of time. In [9], we showed that the time optimal synthesis of the trilinear Hamiltonian $\frac{\pi}{4}4I_{1z}I_{2z}I_{3x}$ takes $\frac{\sqrt{7}}{4J}$ units of time [also see Eq. (16)]. The term $\exp\left(-i\frac{\pi}{4}2I_{1z}I_{3x}\right)$ is locally equivalent to $\sqrt{\mathcal{U}_{13}}=\exp\left(-i\frac{\pi}{4}2I_{1z}I_{3z}\right)$ which can be synthesized in $\frac{4+\sqrt{7}}{4J}=1.66J^{-1}$ units of time, as discussed above [see Fig. 3(B)]. This decomposition results in an overall time for a Toffoli gate of $\frac{5+2\sqrt{7}}{4J}=2.573J^{-1}$ (gate pulse sequence T5).

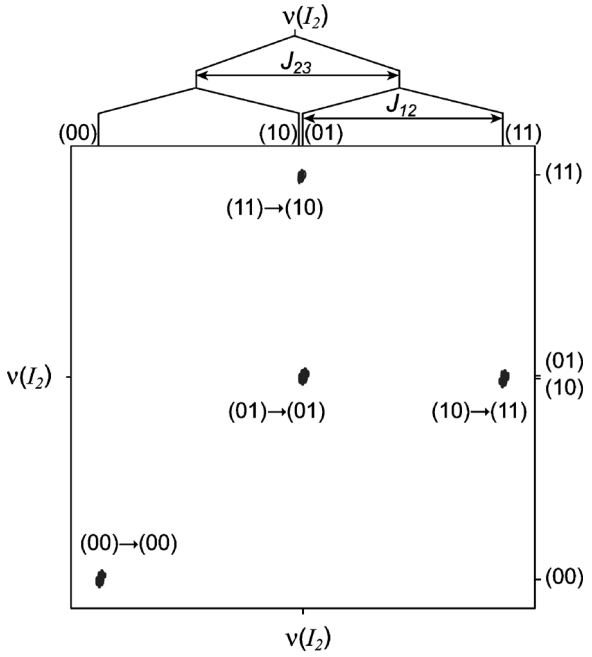

FIG. 5. Experimental two-dimensional ^{15}N spectrum of ^{15}N acetamide representing the effect of the CNOT(1,3) gate. The resonance of ^{15}N is split in three lines due to coupling to spin I_1 and I_3 as shown on top of the figure. The label $(1,0)$ represents the resonance line of spin I_2 when spin I_1 is in state 1 and spin I_3 is in the state 0. In the experiment shown in the figure, the spin I_2 precesses for time t_1 followed by application of the CNOT(1,3) gate, followed by recording the precession of spin I_2 as a function of time real time t_2. The experiment is repeated by incrementing t_1. The two-dimensional signal $s(t_1,t_2)$ is then Fourier transformed and the Larmor frequency of various resonances of spin I_2 during the time t_1 and t_2 are plotted along vertical and horizontal axis, respectively. Using the relation $\text{CNOT}(1,3)=\exp\{-i\frac{\pi}{2}(I_{1z}-I_{3z})\}\times\exp\{-i\frac{\pi}{2}I_{3x}\}\mathcal{U}_{13}\exp\{-i\frac{\pi}{2}I_{3y}\}$, the experimental pulse sequence was based on the implementation of the propagator $\mathcal{U}_{13}$ shown in Fig. 3(A).

Further time savings in the synthesis of the Toffoli gate are achieved by the following construction [see Fig. 3(C)], which also uses the optimal creation of trilinear propagators. Let $U_1=\exp[-i\frac{\pi}{2}(2I_{1x}I_{2x}+2I_{2x}I_{3z})]$, $U_2=\exp[-i\frac{\pi}{4}(4I_{1y}I_{2x}I_{3z})]$, $U_3=\exp[-i\frac{\pi}{4}(2I_{1z}I_{2y})]$, and $U_4=\exp[-i\frac{\pi}{4}(2I_{1z}I_{2z}+2I_{2z}I_{3z})]$. Then it can be verified that $\exp(-iH_{toff})=U_1U_2U_3U_1^{\dagger}U_4$. Note that U_2 and U_3 commute and the optimal synthesis of U_2 as mentioned before takes $\sqrt{7}/4J^{-1}$ units of time, while U_1, U_3, and U_4 take $0.5J^{-1}$, $0.25J^{-1}$, and $0.25J^{-1}$ units of time each. The total time for the synthesis is therefore $\frac{6+\sqrt{7}}{4}J^{-1}=2.16J^{-1}$ (gate pulse sequence T6). This is more than four times faster than gate pulse sequence T1 and a factor of 1.46 faster than the optimal implementation of the Sleator-Weinfurter construction (gate pulse sequence T4). It should be pointed out that if one is only interested in finding a unitary transformation with the same truth table (i.e., the same action on the basis state) as the Toffoli gate then even shorter pulse sequences can be found [24].

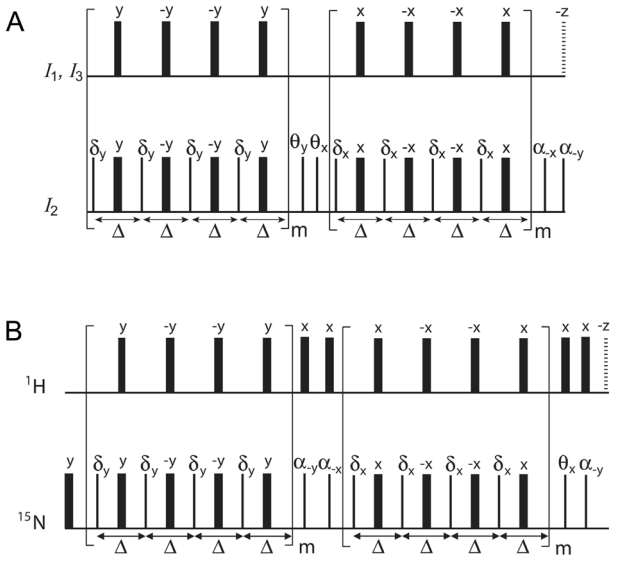

FIG. 6. (A) Broadband version of the ideal U_{13} sequence shown in Fig. 3(A), which is robust with respect to frequency offsets of the spins. Positive coupling constants $J_{12}=J_{23}=J>0$ (with $J_{13}=0$) and hard spin-selective pulses are assumed. The delay Δ is $\tau/(4m)$ and the flip angle δ is $2\pi\nu_a\tau/(4m)=0.5119/m$ (corresponding to $29.33°/m$). (B) Experimentally implemented pulse sequence synthesizing $\mathcal{U}_{13}$ for the spin system of ^{15}N acetamide with $J(^1\text{H},^{15}\text{N})\approx-88$ Hz, $m=2$, flip angles $\alpha=148.6°$, $\theta=31.4°$, and $\delta=14.66°$ and delay $\Delta=890.2$ μs. Narrow and wide bars correspond to 90° and 180° pulses, respectively, if no other flip angle is indicated, z rotations are represented by dashed bars.

In the following section, an experimental realization of these methods on a linear 3 spin chain with Ising couplings is presented.

IV. EXPERIMENT

In Fig. 3, schematic representations of the pulse sequences based on sub-Riemannian geodesics are shown for the efficient implementation of $\mathcal{U}_{13}$ and $\sqrt{\mathcal{U}_{13}}$ simulating coupling evolution by angles $\frac{\pi}{2}$ [Fig. 3(A)] and $\frac{\pi}{4}$ [Fig. 3(B)] between indirectly coupled qubits. As shown above, it is straightforward to construct the CNOT(1,3) gate from $\mathcal{U}_{13}$, which differ only by local rotations. Based on $\sqrt{\mathcal{U}_{13}}$, it is also possible to construct an efficient implementation of the Toffoli gate [Fig. 3(C)]. For simplicity, in Fig. 3 it is assumed that qubits I_1, I_2, and I_3 are on-resonance in their respective rotating frames, coupling constants are positive ($J_{12}=J_{23}=J>0$ and $J_{13}=0$), and hard spin-selective pulses (of negligible duration) are available. More realistic pulse sequences which compensate off-resonance effects by refocusing pulses and practical pulse sequences are given in Section VI.

For an experimental demonstration of the proposed pulse sequence elements, we chose the amino moiety of ^{15}N acetamide (NH_2COCH_3) dissolved in DMSO-d_6 [25]. NMR experiments were performed at a temperature of 295 K using a Bruker 500-MHz Avance spectrometer. Spins I_1 and I_3 are represented by the amino ^{1}H nuclear spins and spin I_2 corresponds to the ^{15}N nuclear spin. The scalar couplings of

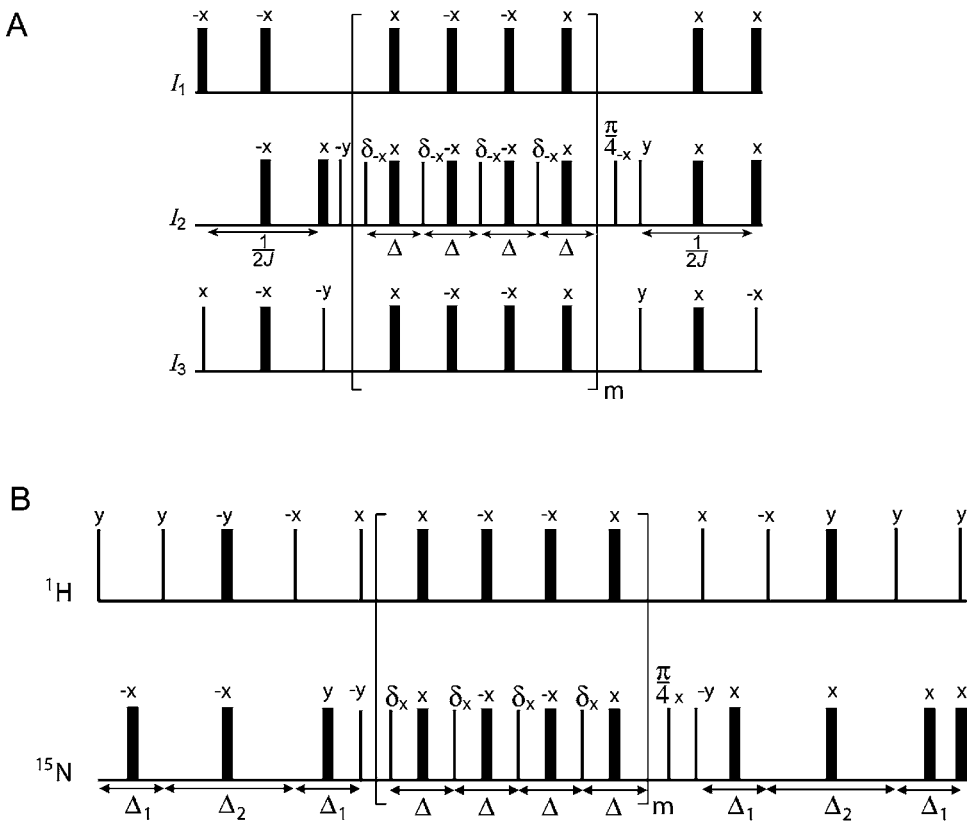

FIG. 7. (A) Broadband version of the ideal $\sqrt{\mathcal{U}_{13}}$ sequence shown in Fig. 3(B), which is robust with respect to frequency offsets of the spins. Positive coupling constants $J_{12}=J_{23}=J>0$ (with $J_{13}=0$) and hard spin-selective pulses are assumed. The delay Δ is $\sqrt{7}/(16mJ)=0.1654/(mJ)$ and the flip angle δ is $3\pi/(8m)$ (corresponding to $67.5°/m$). (B) Experimentally implemented pulse sequence synthesizing $\sqrt{\mathcal{U}_{13}}$ for the spin system of ^{15}N acetamide with $J(^1\mathrm{H},^{15}\mathrm{N})\approx-88$ Hz, $\exp\{-i(\pi/2)I_{1z}I_{3z}\}$ for $J(^1\mathrm{H},^{15}\mathrm{N})\approx-88$ Hz with $m=2$, $\delta=33.75°$, $\Delta=\sqrt{7}/[16m|J(^1\mathrm{H},^{15}\mathrm{N})|]=939.5$ μs, $\Delta_1=1/(4\Delta\nu_{13})=806.5$ μs, and $\Delta_2=1/[2|J(^1\mathrm{H},^{15}\mathrm{N})|]=5.68$ ms.

interest are $J_{12}=-87.3$ Hz$\approx J_{23}=-88.8$ Hz$\gg J_{13}=2.9$ Hz. The actual pulse sequences implemented on the spectrometer and further experimental details are given in the supplementary material.

The propagators of the constructed pulse sequences were tested numerically and we also performed a large number of experimental tests. For example, Fig. 4 shows a series of simulated and experimental ^{1}H spectra of the amino moiety of ^{15}N acetamide. In the simulations, the experimentally determined coupling constants and resonance offsets of the spins were taken into account. The various propagators were calculated for the actually implemented pulse sequences (given in the supplementary material) neglecting relaxation effects. In the simulated spectra, a line broadening of 3.2 Hz was applied in order to facilitate the comparison with the experimental spectra. Starting at thermal equilibrium (in the high-temperature limit), the state $\rho_A=I_{1x}$ can be conveniently prepared by saturating spins I_2 and I_3 (i.e., by creating equal populations of the states $|000\rangle$, $|001\rangle$, $|010\rangle$, $|001\rangle$ and equal populations of the states $|100\rangle$, $|101\rangle$, $|110\rangle$, $|101\rangle$, see Fig. 2) and applying a 90°_y pulse to spin I_1, where ρ_A is the traceless part of the density operator [18]. The resulting spectrum with an absorptive in-phase signal of spin I_1 is shown in Fig. 4(A).

Application of the propagator $U_{13}=\exp\{-i\frac{\pi}{2}2I_{1z}I_{3z}\}$ to ρ_A results in the state $\rho_B=2I_{1y}I_{3z}$. The corresponding spectrum [18] shows dispersive signal of spin I_1 in antiphase with respect to spin I_3, see Fig. 4(B).

The propagator $\sqrt{U_{13}}=\exp\{-i\frac{\pi}{4}2I_{1z}I_{3z}\}$ transforms the prepared state ρ_A into $\rho_C=\frac{1}{\sqrt{2}}(I_{1x}+2I_{1y}I_{3z})$, resulting in a superposition of absorptive in-phase and dispersive antiphase signals of spin I_1, see Fig. 4(C).

The Toffoli gate applied to ρ_A yields

$$\rho_D=\frac{1}{\sqrt{2}}(I_{1x}+2I_{1x}I_{2z}+2I_{1x}I_{3x}-4I_{1x}I_{2z}I_{3x}). \tag{20}$$

Only the first two terms in ρ_D give rise to detectable signals. The corresponding spectrum is a superposition of an absorptive in-phase signal of spin I_1 and an absorptive antiphase signal of spin I_1 with respect to spin I_2, resulting in the spectrum shown in Fig. 4(D).

The effect of the CNOT(1,3) gate can be conveniently demonstrated by using a two-dimensional experiment [26]. Figure 5 shows the resulting two-dimensional spectrum of the ^{15}N multiplet (corresponding to spin I_2) which reflects the expected transformations of the spin states of I_1 and I_3 under the CNOT(1,3) operation.

V. CONCLUSION

In this paper, we have shown that problems of efficient synthesis of couplings between indirectly coupled qubits can be solved by reducing them to problems in geometry. We have constructed efficient ways of synthesizing quantum gates on a linear spin chain with Ising couplings including CNOT and Toffoli operations. We showed significant savings in time in implementing these quantum gates over state-of-the-art methods. The mathematical methods presented here are expected to have applications to broad areas of quantum information technology. The quantum gate design metric $\frac{|dw|^2}{1-|w|^2}$ defined on a open unit disk in a complex plane could play an interesting role in the subject of quantum information.

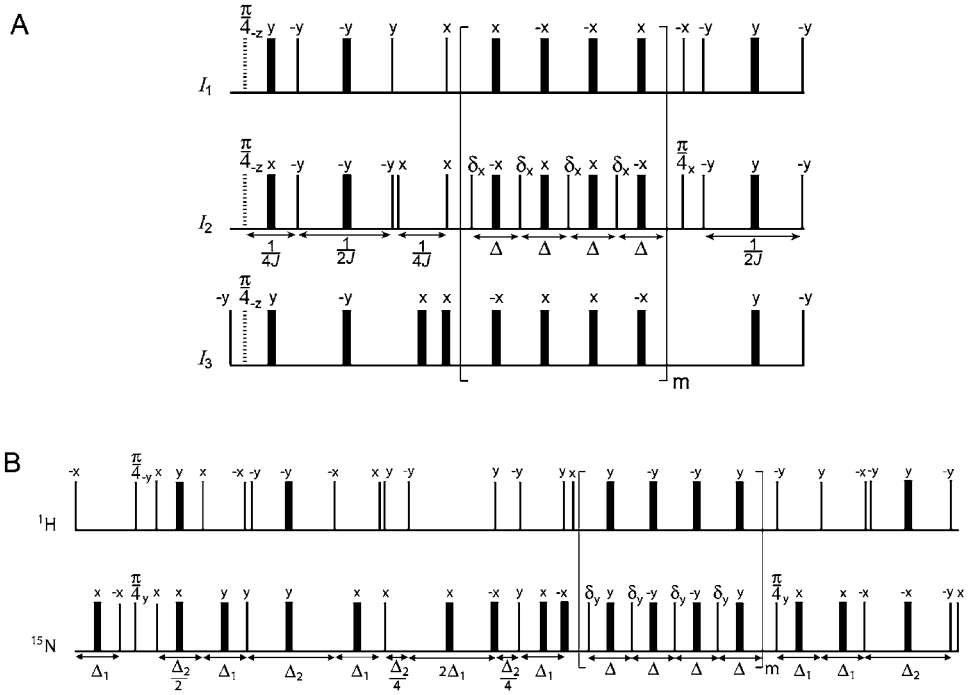

FIG. 8. (A) Broadband version of the ideal Toffoli sequence shown in Fig. 3(C), which is robust with respect to frequency offsets of the spins. Positive coupling constants $J_{12}=J_{23}=J>0$ (with $J_{13}=0$) and hard spin-selective pulses are assumed. (B) Experimentally implemented pulse sequence synthesizing a Toffoli gate for the spin system of ^{15}N acetamide. Delays Δ, Δ_1, Δ_2, and the small flip angle δ are defined in Fig. 7.

The methods presented are expected to have applications to recent proposals of making nuclear spins act as client qubits [17] share information efficiently via distributed hyperfine coupling to an electron spin $\frac{1}{2}$ acting as the bus qubit. Efficient synthesis of couplings between indirectly coupled spins will also be very useful in multidimensional NMR applications to correlate the frequencies of spins 1 and 3 coupled indirectly through spin 2 [18]. Recent numerical optimization studies [27,28] indicate that the gap between conventional and time optimal methods for the synthesis of typical quantum circuits (for, e.g., quantum Fourier transform), on practical architectures, increases rapidly with the number of qubits. This motivates further mathematical developments along the lines of the present work in searching for time optimal techniques of manipulating coupled spin systems. In practical quantum computing, this might prove to be very important as minimizing decoherence losses by efficient gate synthesis improves the fidelity of gates. Since fault tolerant quantum computing protocols require gates to have a fidelity above a certain threshold, optimal gate synthesis methods as presented here could prove critical in practical quantum computing. The problem of constrained optimization that arises in time optimal synthesis of unitary transformations in spin networks is also expected to instigate new ideas and method development in the fields of optimal control and geometry.

VI. SUPPORTING INFORMATION

The ^{1}H and ^{15}N transmitter frequencies were set on resonance for spins I_1 and I_2, respectively. The frequency difference between spins I_1 and I_3 was $\Delta\nu_{13}=310$ Hz. Selective rotations of the ^{15}N nuclear spin I_2 were implemented using hard pulses. Spin-selective proton pulses were realized by combinations of hard pulses and delays in our experiments. For example, a selective 90° rotation of spin I_3 with phase y, denoted $90^\circ_y(I_3)$, is realized by the sequence element $90^\circ_x(I_1,I_3)-(\Delta_1/2)-180^\circ_x(I_2)-(\Delta_1/2)-180^\circ_x(I_2)90^\circ_{-x}(I_1,I_3)$, where $\Delta_1=1/(4\Delta\nu_{13})$ and $90^\circ_{\pm x}(I_1,I_3)$ correspond to nonselective (hard) proton pulses, acting simultaneously on I_1 and I_3. Figures 6(A), 7(A), and 8(A) show broadband versions of the ideal sequence shown in Fig. 3, which are robust with respect to frequency offsets of the spins. Positive coupling constants $J_{12}=J_{23}=J>0$ (with $J_{13}=0$) and hard spin-selective pulses are assumed. Figures 6(B), 7(B), and 8(B) show the actual pulse sequences used in the experiments with the ^{15}N acetamide model system. In the experimental pulse sequences, selective ^{1}H pulses were implemented using hard pulses and delays, where $\Delta_1=1/(4\Delta\nu_{13})$. Furthermore, the sequences were adjusted to take into account that in the experimental model system the couplings J_{12} and J_{23} are negative. Broadband implementations of weak irradiation periods [25] are enclosed in brackets and the number m of repetitions was two in all experiments.

ACKNOWLEDGMENTS

N.K.'s work was supported by a Bessel Prize from the Humboldt Foundation and Research Grants No. ONR 38A-1077404, No. AFOSR FA9550-05-1-0443, and No. AFOSR FA9550-04-1-0427. S.J.G.'s work was supported by the European integrated program QAP and the Bavarian NMR Center.

[1] P. W. Shor, *Proceedings of the 35th Annual Symposium on Fundamentals of Computer Science* (IEEE Press, Los Alamitos, CA, 1994).
[2] M. A. Nielsen and I. L. Chuang, *Quantum Information and Computation* (Cambridge University Press, Cambridge, England, 2000).
[3] M. A. Nielsen, M. R. Dowling, M. Gu, and A. C. Doherty, Science **311**, 1133 (2006).
[4] L. M. K. Vandersypen and I. L. Chuang, Rev. Mod. Phys. **76**, 1037 (2004).
[5] N. Khaneja, R. W. Brockett, and S. J. Glaser, Phys. Rev. A **63**, 032308 (2001).
[6] T. O. Reiss, N. Khaneja, and S. J. Glaser, J. Magn. Reson. **154**, 192 (2002).
[7] H. Yuan and N. Khaneja, Phys. Rev. A **72**, 040301(R) (2005).
[8] G. Vidal, K. Hammerer, and J. I. Cirac, Phys. Rev. Lett. **88**, 237902 (2002).
[9] N. Khaneja, S. J. Glaser, and R. Brockett, Phys. Rev. A **65**, 032301 (2002).
[10] N. Khaneja, F. Kramer, and S. J. Glaser, J. Magn. Reson. **173**, 116 (2005).
[11] N. Khaneja and S. J. Glaser, Phys. Rev. A **66**, 060301(R) (2002).
[12] R. W. Brockett, in *New Directions in Applied Mathematics*, edited by P. Hilton and G. Young (Springer-Verlag, New York, 1981).
[13] J. Baillieul, Ph.D. thesis, Harvard University, Cambridge, MA, 1975.
[14] R. Montgomery, *A Tour of Subriemannian Geometries, their Geodesics and Applications* (American Mathematical Society, Providence, 2002).
[15] B. E. Kane, Nature (London) **393**, 133 (1998).
[16] F. Yamaguchi and Y. Yamamoto, Appl. Phys. A: Mater. Sci. Process. **68**, 1 (1999).
[17] M. Mehring, J. Mende, and W. Scherer, Phys. Rev. Lett. **90**, 153001 (2003).
[18] R. R. Ernst, G. Bodenhausen, and A. Wokaun, *Principles of Nuclear Magnetic Resonance in One and Two Dimensions* (Clarendon, Oxford, 1987).
[19] T. Toffoli, Math. Syst. Theory **14**, 13 (1981).
[20] T. Sleator and H. Weinfurter, Phys. Rev. Lett. **74**, 4087 (1995).
[21] D. P. DiVincenzo, Proc. R. Soc. London, Ser. A **1969**, 261 (1998).
[22] James W. Anderson, *Hyperbolic Geometry* (Springer-Verlag, London, 2001).
[23] D. Collins, K. W. Kim, W. C. Holton, H. Sierzputowska-Gracz, and E. O. Stejskal, Phys. Rev. A **62**, 022304 (2000).
[24] D. Cory *et al.*, Physica D **120**, 82 (1998).
[25] T. O. Reiss, N. Khaneja, and S. J. Glaser, J. Magn. Reson. **165**, 95 (2003).
[26] Z. L. Mádi, R. Brüschweiler, and R. R. Ernst, J. Chem. Phys. **109**, 10603 (1998).
[27] N. Khaneja, T. Reiss, C. Kehlet, T. Schulte-Herbrüggen, and S. J. Glaser, J. Magn. Reson. **172**, 296 (2005).
[28] T. Schulte-Herbrüggen, A. Spörl, N. Khaneja, and S. J. Glaser, Phys. Rev. A **72**, 042331 (2005).